Supplement of Atmos. Chem. Phys., 17, 4319–4336, 2017
http://www.atmos-chem-phys.net/17/4319/2017/
doi:10.5194/acp-17-4319-2017-supplement

Atmospheric Chemistry and Physics Open Access EGU

Supplement of

Source attribution of black carbon and its direct radiative forcing in China

Yang Yang et al.

Correspondence to: Yang Yang (yang.yang@pnnl.gov) and Hailong Wang (hailong.wang@pnnl.gov)

Table S1. Comparison of CEDS annual mean anthropogenic BC emissions in China with those used in other studies

	Year	Anthropogenic emission in China (Gg/yr)
CEDS (Hoesly et al., 2016; this study)	2010–2014 (2010/2014)	2467 (2340/2511)
MIX (Li et al., 2017)	2010	1765
HTAP V2.2 (Janssens-Maenhout et al., 2015)	2010	1741
Lu et al. (2011)	2010	1751
Qin and Xie (2012)	2009	1764
Wang et al. (2012)	2007	1879
INTEX-B (Zhang et al., 2009)	2006	1811

Table S2. Comparisons of observed and modeled seasonal mean near-surface concentrations (units: μg m^{-3}) of BC in China corresponding to Fig. 3a. Numbers in bold represent sites with observed concentration lower than modeled concentration, otherwise the observation higher than modeled concentration.

		DJF		MAM		JJA		SON	
	Sites	Obs.	Model	Obs.	Model	Obs.	Model	Obs.	Model
NC	Gucheng	1.687E+01	6.511E+00	6.939E+00	3.629E+00	7.038E+00	3.403E+00	1.155E+01	4.734E+00
	Linan	**4.831E+00**	**6.175E+00**	4.167E+00	2.952E+00	3.735E+00	1.975E+00	4.133E+00	3.454E+00
	Zhengzhou	1.270E+01	1.054E+01	8.034E+00	4.262E+00	6.939E+00	3.412E+00	9.894E+00	5.486E+00
SC	Jinsha	**3.436E+00**	**7.684E+00**	**2.241E+00**	**3.364E+00**	**1.892E+00**	**2.293E+00**	4.283E+00	4.250E+00
	Panyu	9.628E+00	6.110E+00	8.134E+00	2.832E+00	4.847E+00	1.676E+00	7.437E+00	4.071E+00
	Taiyangshan	**2.623E+00**	**8.352E+00**	**2.042E+00**	**3.750E+00**	**2.092E+00**	**2.428E+00**	**3.652E+00**	**5.001E+00**
SW	Chengdu	1.147E+01	9.194E+00	1.072E+01	2.868E+00	9.728E+00	2.432E+00	1.106E+01	3.776E+00
	Nanning	4.980E+00	4.328E+00	2.623E+00	1.568E+00	2.722E+00	7.740E-01	4.980E+00	2.286E+00
CW	Gaolanshan	5.279E+00	2.556E+00	2.789E+00	9.210E-01	2.872E+00	8.440E-01	4.050E+00	1.326E+00
	Xian	1.853E+01	7.719E+00	1.145E+01	2.863E+00	7.570E+00	2.315E+00	1.077E+01	3.735E+00
NE	Dalian	7.520E+00	1.855E+00	4.548E+00	1.515E+00	3.519E+00	1.183E+00	5.428E+00	1.288E+00
	TYS	3.818E+00	2.604E+00	1.527E+00	1.274E+00	1.112E+00	1.106E+00	2.507E+00	1.774E+00
NW	Dunhuang	5.760E+00	1.960E-01	2.556E+00	9.700E-02	3.436E+00	1.080E-01	4.548E+00	1.510E-01
TP	Lhasa	5.428E+00	1.330E-01	3.021E+00	2.470E-01	3.469E+00	7.700E-02	3.486E+00	1.370E-01

Table S3. Comparisons of observed and modeled seasonal mean aerosol absorption optical depth (AAOD) of BC in China corresponding to Fig. 3b. Numbers in bold represent sites with observed concentration lower than modeled concentration, otherwise the observation higher than modeled concentration. Lack data show in blank.

		DJF		MAM		JJA		SON	
	Sites	Obs.	Model	Obs.	Model	Obs.	Model	Obs.	Model
NC	Beijing	6.430E-02	3.197E-02	5.568E-02	3.280E-02	4.286E-02	3.907E-02	5.303E-02	3.386E-02
	Xianghe	6.658E-02	3.197E-02	5.646E-02	3.280E-02	**3.480E-02**	**3.907E-02**	6.412E-02	3.386E-02
	Xinglong	3.535E-02	3.197E-02	**3.249E-02**	**3.280E-02**	**2.612E-02**	**3.907E-02**	**2.531E-02**	**3.386E-02**
	Taihu	**4.684E-02**	**8.180E-02**	**4.122E-02**	**5.197E-02**	**3.581E-02**	**3.614E-02**	**4.073E-02**	**4.961E-02**
	Hefei	**6.600E-02**	**9.501E-02**	**3.700E-02**	**5.392E-02**			**4.050E-02**	**5.490E-02**
	Shouxian	**6.400E-02**	**9.566E-02**	**2.700E-02**	**5.742E-02**	**2.300E-02**	**4.227E-02**	**4.967E-02**	**5.648E-02**
SC	Chen-Kung U.	**1.468E-02**	**2.629E-02**	1.903E-02	1.659E-02	7.186E-03	1.827E-02	**8.059E-03**	**1.871E-02**
	Polytechnic U.	3.642E-02	3.237E-02	3.790E-02	2.232E-02	5.125E-02	7.519E-03	3.863E-02	1.533E-02
	Hok Tsui	**3.733E-02**	**3.908E-02**	4.733E-02	2.244E-02	4.500E-02	8.432E-03	2.500E-02	1.914E-02
CW	SACOL	**3.047E-02**	**3.908E-02**	3.171E-02	2.244E-02	2.459E-02	8.432E-03	2.288E-02	1.914E-02

Table S4. Contributions from tagged source regions (S, column) to regional mean surface concentrations of BC (μg m^{-3}) over the seven receptor regions in China and China (R, row) in December-January-February (DJF), March-April-May (MAM), June-July-August (JJA), and September-October-November (SON).

DJF								
S \ R	NC	SC	SW	CW	NE	NW	TP	CN
NC	6.305E+00	1.785E+00	1.189E+00	4.652E-01	1.368E-01	3.229E-04	1.999E-02	1.334E+00
SC	1.424E-01	2.931E+00	9.177E-01	7.200E-02	1.080E-03	8.383E-05	1.955E-02	4.472E-01
SW	5.575E-02	1.066E-01	2.218E+00	2.939E-01	1.242E-03	3.116E-04	2.019E-02	2.529E-01
CW	1.091E-01	5.289E-02	9.843E-02	1.124E+00	7.032E-03	3.422E-03	1.645E-03	1.251E-01
NE	5.301E-02	8.742E-03	2.562E-03	8.422E-04	1.028E+00	1.154E-05	4.355E-05	1.558E-01
NW	9.845E-03	5.277E-03	5.362E-03	3.173E-02	2.295E-03	2.730E-01	4.109E-04	6.798E-02
TP	2.466E-03	1.016E-02	4.302E-02	5.238E-03	3.434E-05	1.512E-03	8.590E-02	2.260E-02
RW	4.982E-02	1.843E-01	2.811E-01	3.733E-02	2.785E-02	6.202E-02	2.000E-01	1.135E-01
MAM								
NC	2.805E+00	3.413E-01	1.224E-01	1.069E-01	1.482E-01	1.353E-03	1.098E-03	5.077E-01
SC	1.405E-01	1.612E+00	1.971E-01	1.726E-02	2.537E-03	1.921E-04	2.133E-03	2.239E-01
SW	3.560E-02	3.817E-02	9.879E-01	1.214E-01	1.425E-03	6.528E-04	3.017E-03	1.116E-01
CW	3.417E-02	7.215E-03	1.900E-02	4.112E-01	3.616E-03	4.081E-03	6.567E-04	4.274E-02
NE	3.007E-02	6.737E-03	1.058E-03	7.113E-04	4.709E-01	7.461E-05	1.701E-05	7.255E-02
NW	3.711E-03	1.174E-03	1.408E-03	1.363E-02	1.388E-03	9.920E-02	1.178E-03	2.504E-02
TP	1.727E-03	5.715E-03	2.701E-02	1.967E-03	8.032E-05	3.287E-04	4.822E-02	1.282E-02
RW	7.400E-02	2.171E-01	3.227E-01	3.109E-02	6.560E-02	4.288E-02	1.953E-01	1.244E-01
JJA								
NC	2.137E+00	3.952E-02	2.843E-02	1.073E-01	2.050E-01	2.311E-03	6.508E-04	3.715E-01
SC	2.557E-01	1.205E+00	8.274E-02	2.817E-02	1.588E-02	6.437E-04	1.490E-03	1.878E-01
SW	3.174E-02	1.729E-02	8.374E-01	1.837E-01	5.245E-03	3.773E-03	7.675E-03	1.019E-01
CW	1.413E-02	3.839E-04	4.210E-03	3.078E-01	4.949E-03	8.763E-03	1.428E-03	3.056E-02
NE	1.437E-02	1.215E-04	6.515E-05	1.003E-03	3.823E-01	9.126E-05	1.088E-05	5.674E-02
NW	1.488E-03	1.706E-04	4.902E-04	7.352E-03	1.217E-03	7.450E-02	6.138E-03	1.926E-02
TP	6.764E-04	4.352E-04	1.231E-02	1.712E-03	8.545E-05	2.180E-04	2.878E-02	6.962E-03
RW	6.458E-02	1.118E-01	7.125E-02	2.073E-02	6.657E-02	4.698E-02	5.019E-02	6.049E-02
SON								
NC	3.637E+00	6.013E-01	3.029E-01	1.583E-01	2.115E-01	9.076E-04	7.141E-03	6.949E-01
SC	1.054E-01	2.069E+00	4.831E-01	3.467E-02	1.079E-03	1.157E-04	1.368E-02	2.999E-01
SW	2.732E-02	2.834E-02	1.337E+00	1.643E-01	1.892E-03	1.094E-03	1.921E-02	1.481E-01
CW	4.850E-02	1.661E-02	2.963E-02	5.772E-01	9.169E-03	6.773E-03	8.261E-04	6.189E-02
NE	3.755E-02	1.131E-02	3.194E-03	1.005E-03	7.166E-01	5.863E-05	9.987E-05	1.094E-01
NW	8.370E-03	3.558E-03	3.133E-03	2.469E-02	4.048E-03	1.642E-01	2.925E-03	4.264E-02
TP	1.286E-03	2.176E-03	2.050E-02	2.855E-03	6.000E-05	4.644E-04	5.926E-02	1.395E-02
RW	5.646E-02	1.193E-01	6.751E-02	2.109E-02	3.994E-02	5.407E-02	8.808E-02	6.482E-02

Table S5. Comparison of the simulated annual mean emission, burden, DRF and DRF efficiency in China in this study with the values reported in three previous studies.

Reference	Model	Year	Emission in China (Gg yr^{-1})	Burden (mg m^{-2})	DRF (Wm^{-2})	DRF efficiency (W m^{-2} Tg^{-1})
Wu et al. (2008)	RegCM3	2000	1005	0.55–1.42	0.64–1.55	0.64–1.55
Zhuang et al. (2011)	RegCCMS	2006	1811	1.12	0.75	0.41
Li et al. (2016)	GEOS-Chem	2010	1840		1.22	0.66
This study	CESM	2010–2014	2497	1.61	2.20	0.88

Table S6. Seasonal and annual direct radiative effect (DRF) efficiency of BC (W m^{-2} Tg^{-1}) for each of the tagged source regions over China and globally, respectively. The efficiency is defined as the DRF divided by the corresponding scaled annual emission (seasonal emission multiplied by 4).

China	DJF	MAM	JJA	SON	ANN
NC	5.178E-01	5.805E-01	6.588E-01	5.636E-01	5.714E-01
SC	4.966E-01	4.349E-01	6.029E-01	6.225E-01	5.344E-01
SW	9.109E-01	8.062E-01	7.083E-01	7.696E-01	8.036E-01
CW	7.545E-01	1.013E+00	1.138E+00	8.336E-01	9.047E-01
NE	2.774E-01	3.576E-01	4.898E-01	2.692E-01	3.324E-01
NW	9.319E-01	1.628E+00	3.029E+00	1.801E+00	1.687E+00
TP	1.144E+00	1.210E+00	8.162E-01	1.001E+00	1.061E+00
Global	DJF	MAM	JJA	SON	ANN
NC	2.276E-02	4.297E-02	3.444E-02	2.317E-02	2.983E-02
SC	2.728E-02	2.542E-02	2.555E-02	2.768E-02	2.643E-02
SW	4.515E-02	4.251E-02	2.818E-02	3.386E-02	3.794E-02
CW	3.010E-02	6.253E-02	5.214E-02	3.321E-02	4.227E-02
NE	1.196E-02	4.104E-02	3.886E-02	1.967E-02	2.609E-02
NW	2.844E-02	8.623E-02	1.344E-01	7.472E-02	7.227E-02
TP	6.105E-02	7.493E-02	4.098E-02	5.296E-02	5.930E-02
RW	5.458E-02	6.606E-02	7.307E-02	7.054E-02	6.632E-02

Table S7. Seasonal and annual near-surface concentration (μg m^{-3} Tg^{-1}) and column burden (mg m^{-2} Tg^{-1}) efficiency of BC for each of the tagged source regions over China and globally, respectively.

			Near-Surface Concentration Efficiency		
China	DJF	MAM	JJA	SON	ANN
NC	8.920E-01	5.195E-01	4.087E-01	7.132E-01	6.667E-01
SC	6.695E-01	4.002E-01	3.378E-01	5.465E-01	4.951E-01
SW	5.371E-01	2.938E-01	2.743E-01	3.971E-01	3.869E-01
CW	7.907E-01	4.275E-01	3.616E-01	5.879E-01	5.843E-01
NE	5.882E-01	3.356E-01	3.898E-01	5.206E-01	4.710E-01
NW	8.737E-01	4.916E-01	4.730E-01	7.950E-01	7.001E-01
TP	4.273E-01	2.102E-01	1.708E-01	3.191E-01	2.840E-01
Global	DJF	MAM	JJA	SON	ANN
NC	2.206E-02	1.314E-02	9.203E-03	1.666E-02	1.617E-02
SC	1.930E-02	9.466E-03	7.600E-03	1.401E-02	1.290E-02
SW	1.456E-02	6.832E-03	5.703E-03	9.447E-03	9.497E-03
CW	1.854E-02	9.932E-03	7.819E-03	1.307E-02	1.338E-02
NE	1.602E-02	1.134E-02	9.942E-03	1.516E-02	1.353E-02
NW	2.223E-02	1.283E-02	1.089E-02	1.987E-02	1.765E-02
TP	1.322E-02	5.877E-03	3.801E-03	8.315E-03	7.933E-03
RW	1.547E-02	1.224E-02	1.192E-02	1.369E-02	1.329E-02
			Column Burden Efficiency		
China	DJF	MAM	JJA	SON	ANN
NC	7.758E-01	5.072E-01	4.046E-01	6.130E-01	6.022E-01
SC	6.344E-01	3.572E-01	3.965E-01	5.321E-01	4.859E-01
SW	7.625E-01	3.701E-01	3.382E-01	4.783E-01	5.057E-01
CW	8.424E-01	5.659E-01	4.951E-01	6.502E-01	6.746E-01
NE	2.526E-01	2.526E-01	3.020E-01	3.009E-01	2.730E-01
NW	5.382E-01	6.537E-01	1.010E+00	9.524E-01	7.537E-01
TP	6.736E-01	3.918E-01	2.661E-01	4.499E-01	4.529E-01
Global	DJF	MAM	JJA	SON	ANN
NC	2.442E-02	2.057E-02	1.345E-02	1.899E-02	2.008E-02
SC	2.402E-02	1.275E-02	1.225E-02	1.814E-02	1.711E-02
SW	2.880E-02	1.483E-02	9.967E-03	1.652E-02	1.826E-02
CW	2.618E-02	2.289E-02	1.671E-02	1.975E-02	2.223E-02
NE	1.142E-02	1.810E-02	1.461E-02	1.617E-02	1.490E-02
NW	1.680E-02	2.685E-02	3.681E-02	3.401E-02	2.701E-02
TP	3.236E-02	2.213E-02	1.129E-02	1.971E-02	2.205E-02
RW	2.733E-02	2.548E-02	2.799E-02	2.881E-02	2.745E-02

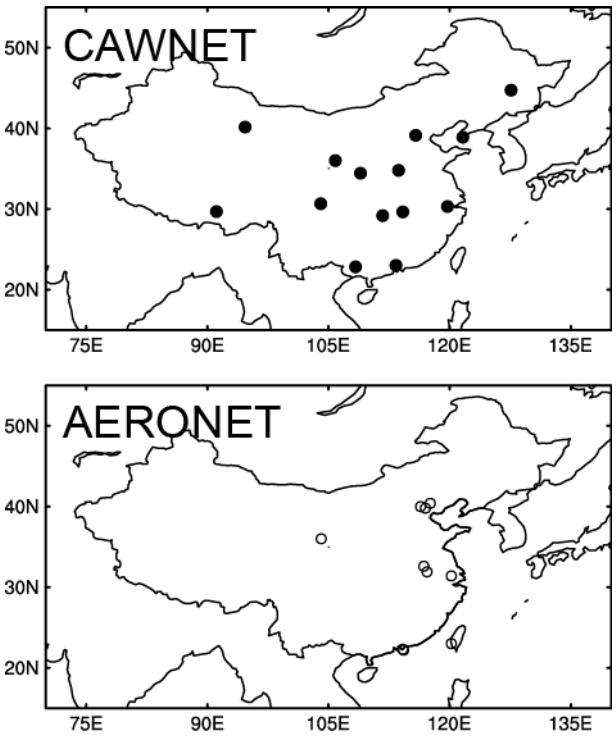

Figure S1. Locations of 14 sites of the China Meteorological Administration (CMA) Atmosphere Watch Network (CAWNET, top) (Zhang et al., 2012) and 10 sites of the Aerosol Robotic Network (AERONET, bottom) (Holben et al., 2001).

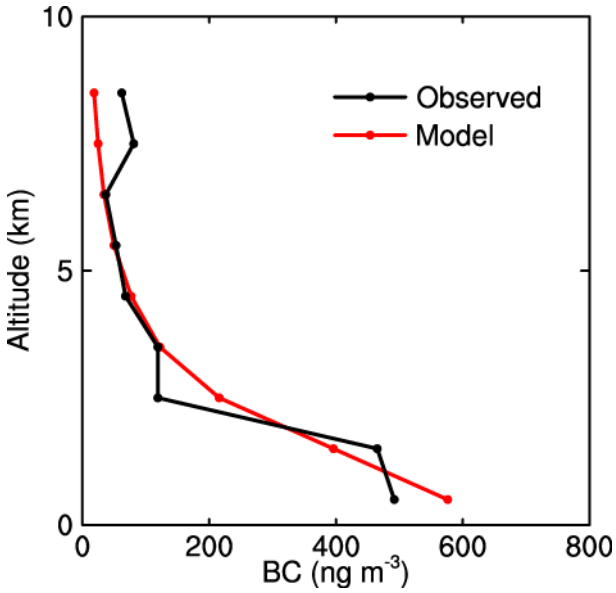

Figure S2. Observed and simulated mean vertical profiles of BC concentrations in the East-Asian outflow region. The observed BC profile is from the A-FORCE field campaign conducted over the Yellow Sea, the East China Sea, and the western Pacific Ocean in March–April 2009 (Oshima et al., 2012).

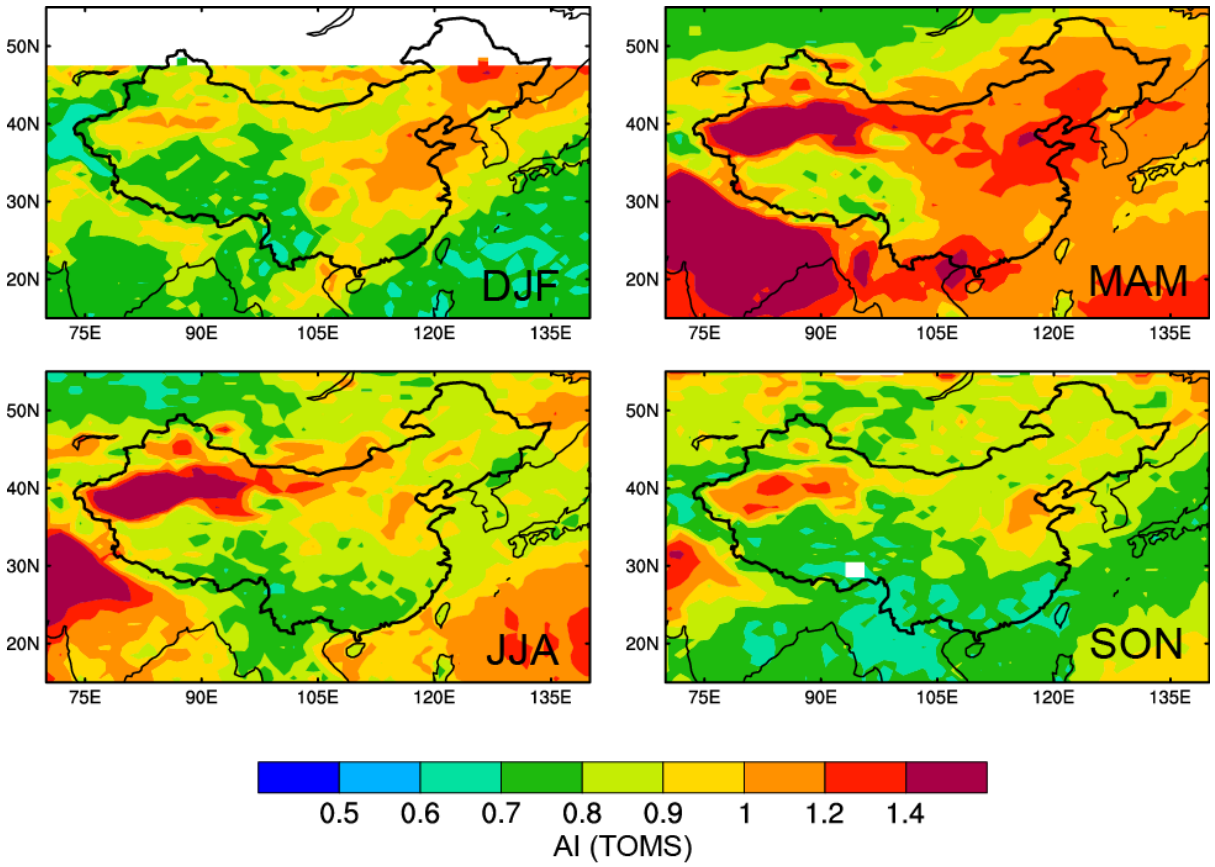

Figure S3. Spatial distribution of seasonal mean Aerosol Index (AI) derived from Total Ozone Mapping Spectrometer (TOMS) measurements over years of 1997–2004.

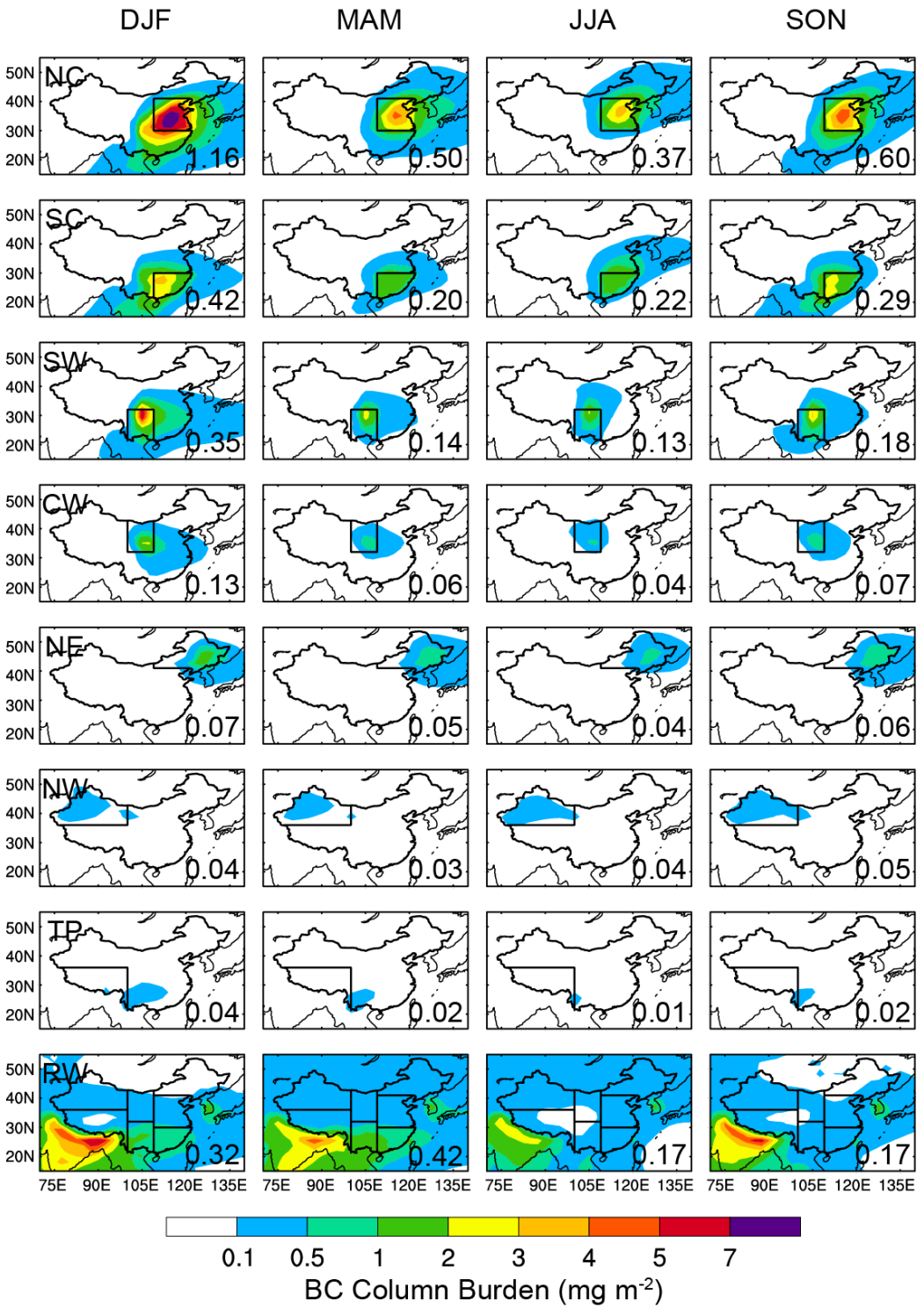

Figure S4. Spatial distribution of seasonal mean BC column burden (mg m^{-2}) originating from the seven source regions in China (NC, SC, SW, CW, NE, NW, and TP), marked with black outlines, and sources outside China (RW). Regionally averaged BC in China contributed by individual source regions is shown at the bottom right of each panel.

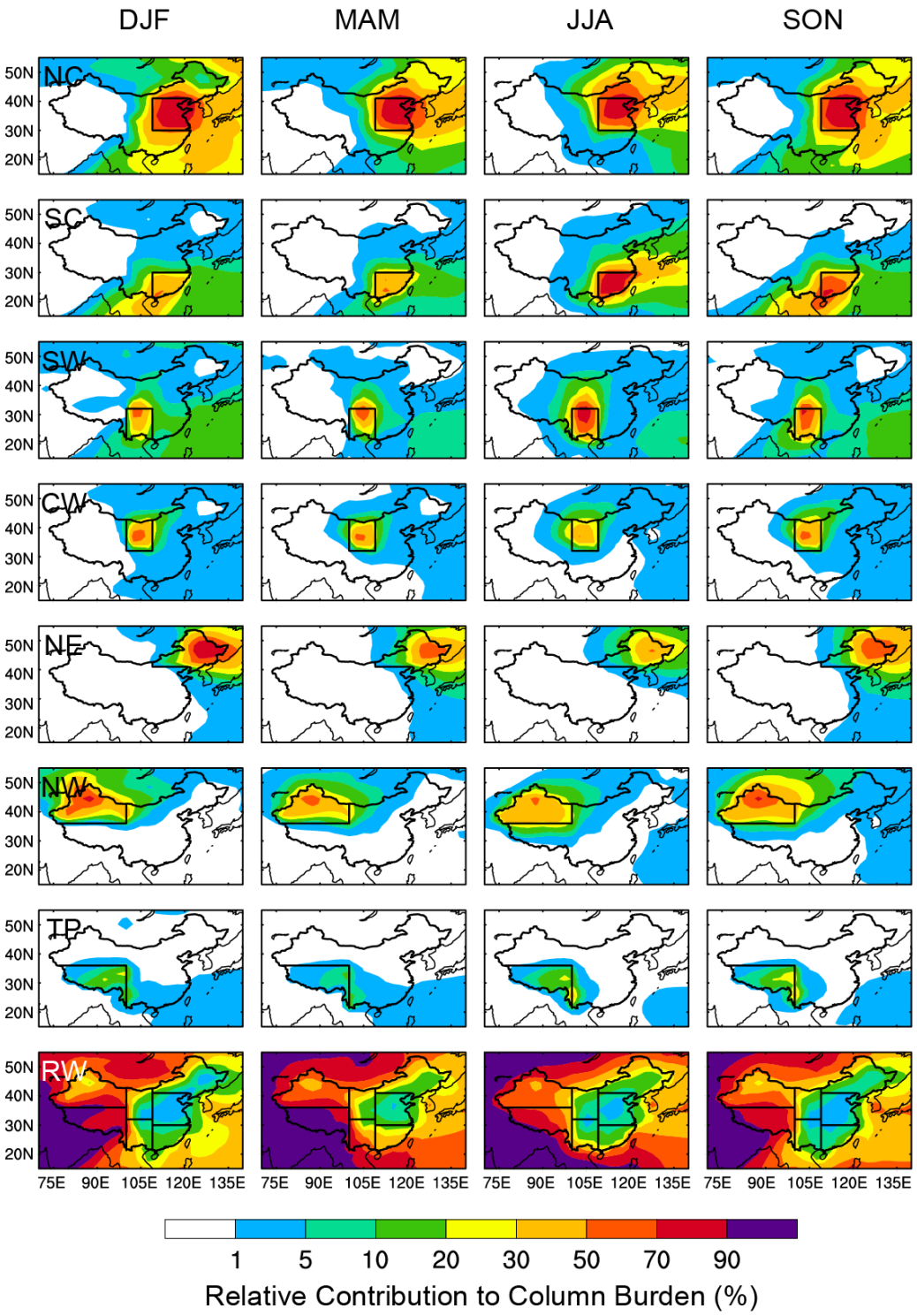

Figure S5. Spatial distribution of relative contributions (%) to seasonal mean BC column burden from each of the tagged source regions.

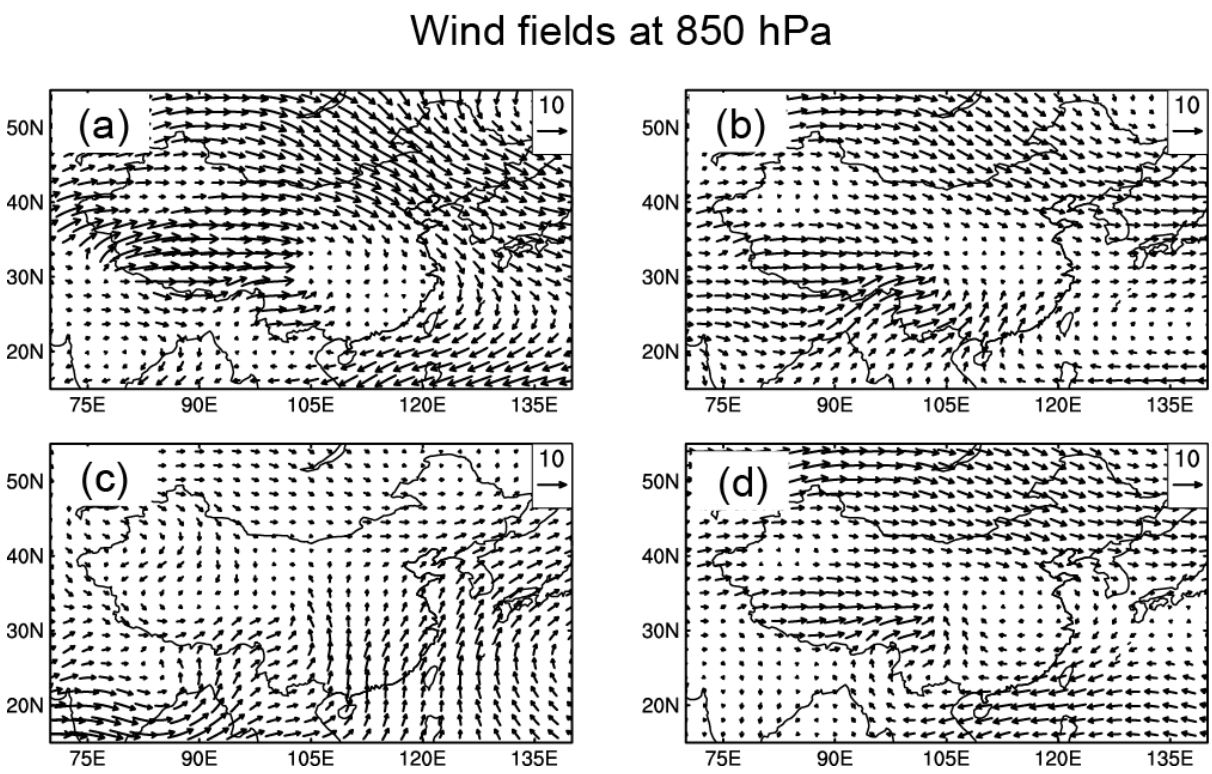

Figure S6. Simulated seasonal mean winds at 850 hPa (m s^{-1}) in (a) December-January-February (DJF), (b) March-April-May (MAM), (c) June-July-August (JJA), and (d) September-October-November (SON).

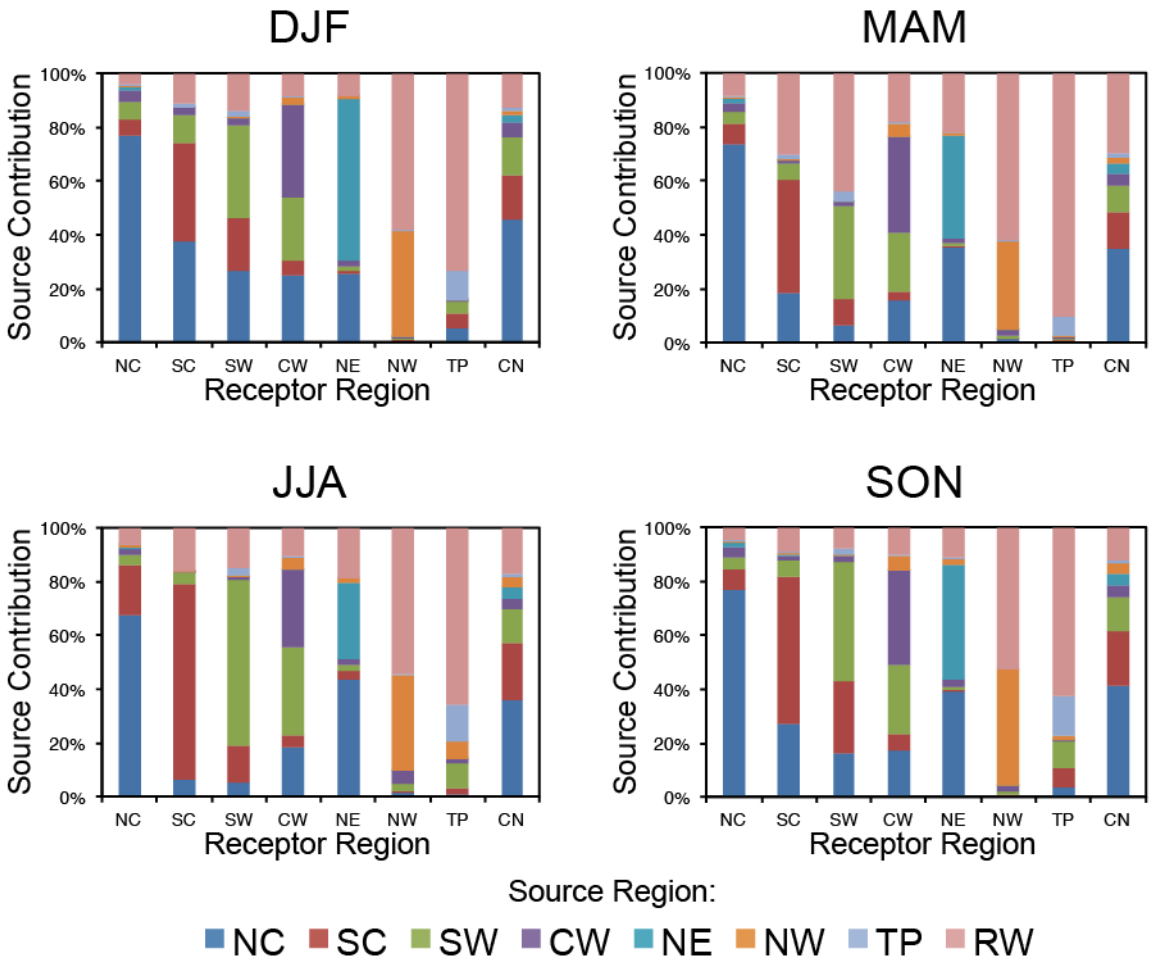

Figure S7. Relative contributions (%) from the tagged source regions (denoted by colors) to regional mean BC column burden over seven receptor regions in China (NC, SC, SW, CW, NE, NW, and TP) and all of China (CN) in different seasons. The receptor regions are marked on the horizontal axis in each panel.

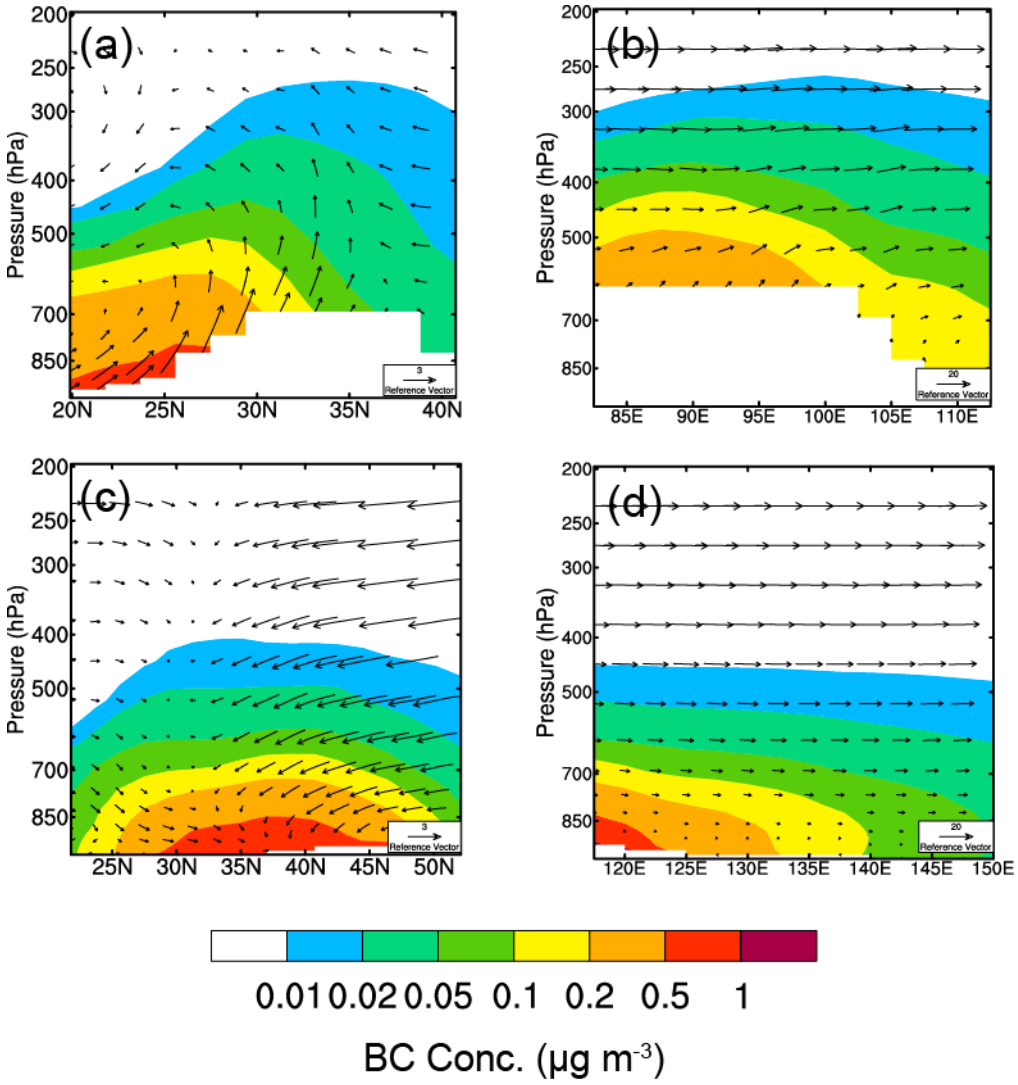

Figure S8. Vertical distributions of BC concentrations (μg m^{-3}), originating from emissions outside China, averaged over (a) 75°–120°E and (b) 25°–35°N, respectively, near the south boundary of China, and BC originating from total emissions in China averaged over (c) 120°–135°E and (d) 20°–50°N, respectively, near the east boundary of China.

Reference

Janssens-Maenhout, G., Crippa, M., Guizzardi, D., Dentener, F., Muntean, M., Pouliot, G., Keating, T., Zhang, Q., Kurokawa, J., Wankmüller, R., Denier van der Gon, H., Kuenen, J. J. P., Klimont, Z., Frost, G., Darras, S., Koffi, B., and Li, M.: HTAP_v2.2: a mosaic of regional and global emission grid maps for 2008 and 2010 to study hemispheric transport of air pollution, Atmos. Chem. Phys., 15, 11411-11432, doi:10.5194/acp-15-11411-2015, 2015.

Li, K., Liao, H., Mao, Y. H., and Ridley, D. A.: Source sector and region contributions to concentration and direct radiative forcing of black carbon in China, Atmos. Environ., 124, 351–366, doi:10.1016/j.atmosenv.2015.06.014, 2016.

Lu, Z., Zhang, Q., and Streets, D. G.: Sulfur dioxide and primary carbonaceous aerosol emissions in China and India, 1996–2010, Atmos. Chem. Phys., 11, 9839-9864, doi:10.5194/acp-11-9839-2011, 2011.

Oshima, N., Kondo, Y., Moteki, N., Takegawa, N., Koike, M., Kita, K., Matsui, H., Kajino, M., Nakamura, H., Jung, J. S., and Kim, Y. J.: Wet removal of black carbon in Asian outflow: Aerosol Radiative Forcing in East Asia (A-FORCE) aircraft campaign, J. Geophys. Res., 117, D03204, doi:10.1029/2011jd016552, 2012.

Qin, Y. and Xie, S. D.: Spatial and temporal variation of anthropogenic black carbon emissions in China for the period 1980–2009, Atmos. Chem. Phys., 12, 4825-4841, doi:10.5194/acp-12-4825-2012, 2012.

Wang, R., Tao, S., Wang, W., Liu, J., Shen, H., Shen, G., Wang, B., Liu, X., Li, W., Huang, Y., Zhang, Y., Lu, Y., Chen, H., Chen, Y., Wang, C., Zhu, D., Wang, X., Li, B., Liu, W., Ma, J.: Black carbon emissions in China from 1949 to 2050, Environ. Sci. Technol., 46, 7595-7603, doi:10.1021/es3003684, 2012.

Zhang, Q., Streets, D. G., Carmichael, G. R., He, K. B., Huo, H., Kannari, A., Klimont, Z., Park, I. S., Reddy, S., Fu, J. S., Chen, D., Duan, L., Lei, Y., Wang, L. T., and Yao, Z. L.: Asian emissions in 2006 for the NASA INTEX-B mission, Atmos. Chem. Phys., 9, 5131-5153, doi:10.5194/acp-9-5131-2009, 2009.